PROCEEDINGS OF SCIENCE

Quark-gluon plasma properties

Georgios K. Krintiras[a,**]

[a] *Department of Physics and Astronomy, The University of Kansas, Malott Hall, 1251 Wescoe Hall Dr., Lawrence, KS 66045, US*
cern.ch/gkrintir

E-mail: gkrintir@cern.ch

Heavy ion collisions are used to study fundamental features of quantum chromodynamics (QCD) matter via its excitation to phases where quarks and gluons are no more confined into hadrons. Studies of the properties of this deconfined quark–gluon matter, called quark–gluon plasma (QGP), at the Brookhaven Relativistic Heavy-Ion Collider and the LHC have shown that the QGP behaves like a liquid with very small specific shear and bulk viscosities, and high opacity for energetic jets. Macroscopic (microscopic) properties are encoded in the collective expansion (underlying parton dynamics) of the strongly interacting QGP. Here, we review recent progress on measurements at the LHC particle production from small to large transverse momentum or mass, jet-induced medium response, heavy quark and exotic meson production, and photon-initiated processes. Increasingly high-precision data, along with novel approaches, offer stringent constraints on initial state, QGP formation and transport parameters, and even parametrizations beyond the standard model.

The Tenth Annual Conference on Large Hadron Collider Physics - LHCP2022
16–20 May 2022
online

*Speaker (on behalf of the ALICE, ATLAS, LHCb and CMS collaborations);supported in whole by DE-FG02-96ER40981.

PoS(LHCP2022)015

1. Introduction

Here, we briefly present the latest results at LHC [1–4] using lead-lead (PbPb) and proton-lead (pPb) collisions, which provide stringent constraints on cold and hot nuclear matter effects [5] (and references therein).

2. Investigating the early stages of the transverse and longitudinal QGP formation

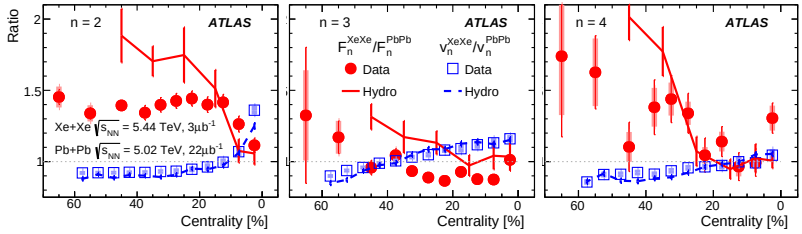

Figure 1: The ratios of flow decorrelation ($F_n^{\mathrm{XeXe}}/F_n^{\mathrm{PbPb}}$) and amplitude ($v_n^{\mathrm{XeXe}}/v_n^{\mathrm{PbPb}}$) variables from data (solid symbols) and models (solid and dashed lines) as a function of centrality for the second- (left), third- (middle), or fourth-order harmonic (right), respectively. The error bars and shaded boxes on the data represent statistical and systematic uncertainties, respectively. The vertical error bars on the theory calculations represent the statistical uncertainties.

So far it was assumed that the shape of the initial overlap and dynamic evolution of the QGP are boost-invariant. To improve our understanding of the QGP longitudinal structure, the ATLAS Collaboration extended the measurements to a broader range in the beam energy and size of the available collision systems [6]. Hydrodynamic models are found to describe the ratios of flow amplitudes between XeXe and PbPb, but fail to describe most of the magnitudes and trends of the ratios of the flow decorrelations between XeXe and PbPb (Fig. 1). This suggests that current models tuned to describe the transverse dynamics do not necessarily describe the longitudinal structure of the initial-state geometry.

3. Extracting QGP thermodynamic properties with state-of-the-art flow observables

Determining the cumulant $v_2\{2k\}$ values of the second order (v_2) flow distribution, where k corresponds to the number of particles used to determine the correlation and labels the order of the cumulant, is an alternative way for understanding whether the momentum anisotropies at low- and intermediate-p_{T} have a common origin due to initial-state fluctuations. A fine splitting is observed by the CMS Collaboration among $v_2\{4\}$, $v_2\{6\}$, $v_2\{8\}$, and $v_2\{10\}$ [7]. This splitting is attributed to a nonGaussian behavior in the event-by-event fluctuations of the v_2 distribution, as shown in Fig. 2 (left). Although extensive measurements of light hadron azimuthal anisotropies have been performed in all collision systems at LHC, open heavy flavor hadrons and quarkonia provide us with information about the interaction of heavy quarks with the medium, including heavy quark

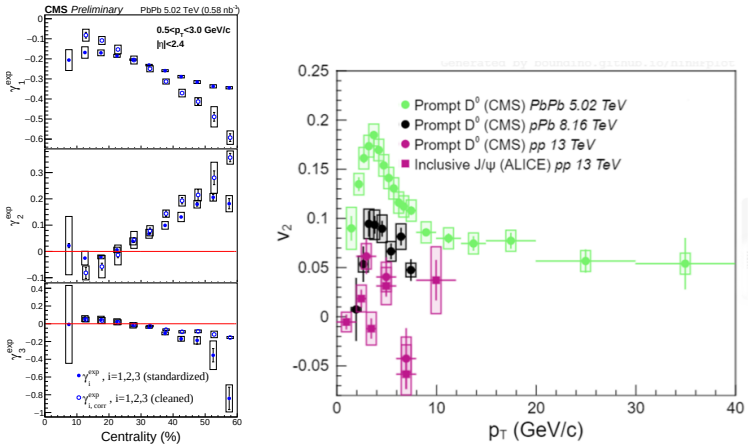

Figure 2: Left: The magnitudes of the experimentally measured before (closed circles) and after accounting for contributions from higher-order moments (open circles) skewness (top), kurtosis (middle), and the superskewness (bottom) as a function of centrality in PbPb collisions at $\sqrt{s_{\mathrm{NN}}} = 5.02\,\mathrm{TeV}$. The bars (open boxes) denote statistical (systematic) uncertainties [7]. Right: Summary of elliptic azimuthal anisotropy coefficient measurements for charm (D^0 [8–10] and J/ψ from the preliminary Ref. [11]) hadrons, using LHC data samples of PbPb, pPb, and pp collisions at different $\sqrt{s_{\mathrm{NN}}}$.

fragmentation and hadron formation processes. They also offer a unique opportunity to disentangle different QCD effects at the boundary between low- and high-p_{T} interactions, and hence shed light on the origin of flow in small collision systems. A selection of the latest measurements at LHC is presented in Fig. 2 (right) for the flow of heavy flavor hadrons.

4. Jets and parton energy loss

The in-medium energy loss, which carries information on the medium properties and expansion, can be also investigated by measuring the R_{AA} of heavy flavor hadrons. This is recently demonstrated by the ALICE Collaboration [12] when measuring the ratio of nonprompt to prompt D^0-meson R_{AA}, found to be significantly larger than unity (Fig. 3, left). Models can describe their ratio as a function of meson p_{T} only once they encoded a quark mass dependence of energy loss, both at high meson p_{T}—where beauty quarks lose less energy than charm quarks via radiative processes—and at low meson p_{T}—a region in which collisional processes are more relevant and the interaction of heavy quarks with the medium can be described as a diffusion process. Access to the hard splittings inside a jet is now possible thanks to jet grooming algorithms that isolate substructures in a well-controlled perturbative QCD framework by removing soft wide-angle radiation. Measurements from ALICE (on the groomed jet radius θ_g [13]) and ATLAS (on the angular scale r_g of the first hard splitting [14] as in Fig. 3, right) collaborations are the first direct comparisons of predictions to fully corrected data, indicating that the degree of incoherent energy loss and the relative quark/gluon suppression are possible physics mechanisms that lead to a suppression of wide-angle splittings.

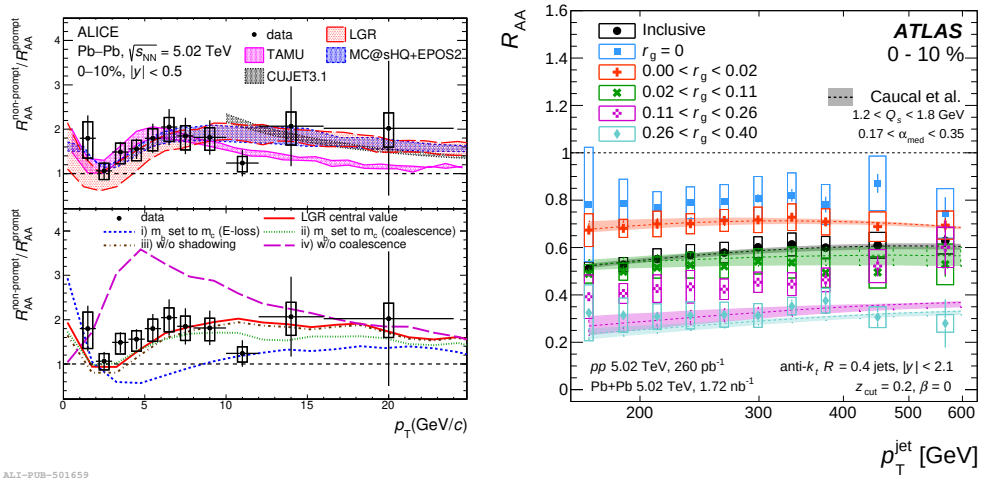

Figure 3: Left: Nonprompt to prompt D^0-meson R_{AA} ratio as a function of meson p_T in the 0–10% central PbPb collisions at $\sqrt{s_{NN}} = 5.02$ TeV, compared to model predictions (top), and to different modifications of calculations including both radiative and collisional energy loss processes (bottom) [12]. Right: Comparison of R_{AA} for inclusive jets and for four intervals of r_g in 0–10% centrality PbPb events to theoretical predictions. The error bars and the open boxes around the data points represent the statistical and systematic uncertainties, respectively [14].

5. Properties of quarkonium and exotic states in the QGP

On the one hand, the availability of increasingly precise experimental results [15, 16], as shown in the left and middle of Fig. 4, for various quarkonium states represents a crucial input for the evaluation of the theory approaches related to sequential suppression and recombination processes. On the other hand, measurements in heavy ion collisions can provide new tests for models of particle transport and hadronization in an extended range of number of constituent quarks. The CMS [17] and LHCb [18] collaborations have performed the first measurements of the exotic X(3872) state in PbPb and pPb collisions, respectively (Fig. 4, right). Interestingly, the increase of the $\sigma_{X(3872)}/\sigma_{\psi(2S)}$ ratio from pp to pPb and PbPb collisions may indicate that the exotic X(3872) hadron experiences different dynamics in the nuclear medium than the conventional charmonium state $\psi(2S)$. These measurements can provide new constraints on the allowed configurations of quarks inside hadrons, as well as models of parton transport and hadronization in nuclear collisions.

6. Summary

In these proceedings, we gave an experimental overview of relevant recent measurements trying to address three guiding questions (nicely put in Ref. [19]): "How does the strongly coupled QGP emerge from an asymptotically free gauge theory"; "What is the (sub)structure of QGP when probed at various resolution scales"; and "What are the QGP transport properties"? It is evident that it will become increasingly important to understand the initial conditions, unify the hydrodynamic description of all available collision systems, and quantify better hadronization [20] to achieve these goals.

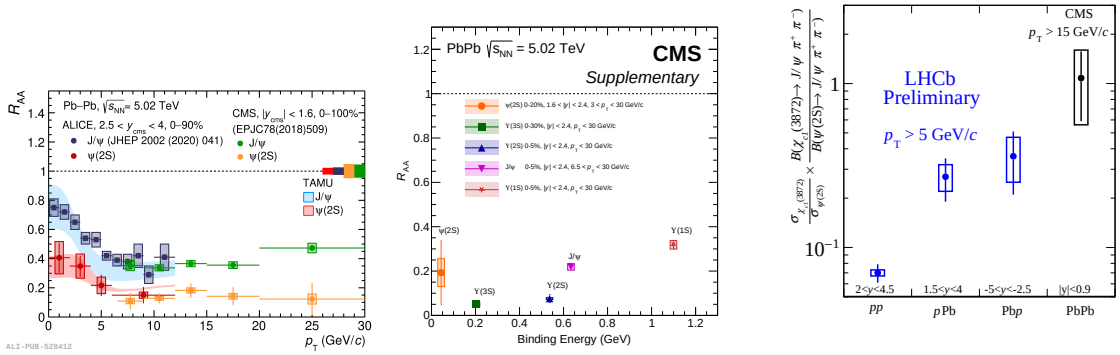

Figure 4: Left:The R_{AA} for ψ(2S) and J/ψ as a function of meson p_T. Comparison with theory models and results from the CMS Collaboration are also shown [15]. Middle: The R_{AA} at $\sqrt{s_{NN}}$ = 5.02 TeV for various quarkonium mesons (ψ(2S), J/ψ, and Υ(nS)) as a function of the quarkonium binding energy. The error bars and boxes represent the statistical and systematic uncertainties, respectively [16]. Right: The $\sigma_{X(3872)}/\sigma_{\psi(2S)}$, measured in pp, pPb, and PbPb collisions. The error bars (boxes) represent the statistical (systematic) uncertainties in the ratio [18].

References

[1] ALICE Collaboration, "Future high-energy pp program with ALICE", ALICE Public Note, 2020.

[2] ATLAS Collaboration, "The ATLAS Experiment at the CERN Large Hadron Collider", *JINST* **3** (2008) S08003, doi:10.1088/1748-0221/3/08/S08003.

[3] CMS Collaboration, "The CMS experiment at the CERN LHC", *JINST* **3** (2008) S08004, doi:10.1088/1748-0221/3/08/S08004.

[4] LHCb Collaboration, "The LHCb Detector at the LHC", *JINST* **3** (2008) S08005, doi:10.1088/1748-0221/3/08/S08005.

[5] G. K. Krintiras (on behalf of the CMS Collaboration), "Review of results using heavy ion collisions at CMS", in *Workshop of QCD and Forward Physics at the the LHC, the future Electron Ion Collider and Cosmic Ray Physics*. University of Kansas Libraries, 2020. arXiv:2006.05556.

[6] ATLAS Collaboration, "Longitudinal flow decorrelations in XeXe collisions at $\sqrt{s_{NN}}$ = 5.44 TeV with the ATLAS detector", *Phys. Rev. Lett.* **126** (2021) 122301, doi:10.1103/PhysRevLett.126.122301, arXiv:2001.04201.

[7] CMS Collaboration, "Probing hydrodynamics and the moments of the elliptic flow distribution in 5.02 TeV lead-lead collisions using higher-order cumulants", CMS Physics Analysis Summary CMS-PAS-HIN-21-010, 2022.

[8] CMS Collaboration, "Measurement of prompt D^0 and $\overline{D}^0$ meson azimuthal anisotropy and search for strong electric fields in PbPb collisions at $\sqrt{s_{NN}} = 5.02$ TeV", *Phys. Lett. B* **816** (2021) 136253, doi:10.1016/j.physletb.2021.136253, arXiv:2009.12628.

[9] CMS Collaboration, "Elliptic flow of charm and strange hadrons in high-multiplicity pPb collisions at $\sqrt{s_{NN}} = 8.16$ TeV", *Phys. Rev. Lett.* **121** (2018) 082301, doi:10.1103/PhysRevLett.121.082301, arXiv:1804.09767.

[10] CMS Collaboration, "Studies of charm and beauty hadron long-range correlations in pp and pPb collisions at LHC energies", *Phys. Lett. B* **813** (2021) 136036, doi:10.1016/j.physletb.2020.136036, arXiv:2009.07065.

[11] ALICE Collaboration, "p_T dependence of J/ψ v_2 in pp collisions at 13 TeV", 2022. https://alice-figure.web.cern.ch/node/22601.

[12] ALICE Collaboration, "Measurement of beauty production via nonprompt D^0 mesons in PbPb collisions at $\sqrt{s_{NN}} = 5.02$ TeV", arXiv:2202.00815. Submitted to *Phys. Rev. Lett.*

[13] ALICE Collaboration, "Measurement of the groomed jet radius and momentum splitting fraction in pp and PbPb collisions at $\sqrt{s_{NN}} = 5.02$ TeV", *Phys. Rev. Lett.* **128** (2022) 102001, doi:10.1103/PhysRevLett.128.102001, arXiv:2107.12984.

[14] ATLAS Collaboration, "Measurement of substructure-dependent jet suppression in PbPb collisions at 5.02 TeV with the ATLAS detector", (2022). arXiv:2211.11470.

[15] ALICE Collaboration, "ψ(2S) suppression in PbPb collisions at the LHC", (2022). arXiv:2210.08893. Submitted to *Phys. Rev. Lett.*

[16] CMS Collaboration, "Observation of the $\Upsilon(3S)$ meson and suppression of Υ states in PbPb collisions at $\sqrt{s_{NN}} = 5.02$ TeV", (2023). arXiv:2303.17026. Submitted to *Phys. Rev. Lett.*

[17] CMS Collaboration, "Evidence for X(3872) in PbPb collisions and studies of its prompt production at $\sqrt{s_{NN}}$=5.02 TeV", *Phys. Rev. Lett.* **128** (2022) 032001, doi:10.1103/PhysRevLett.128.032001, arXiv:2102.13048.

[18] LHCb Collaboration, "Modification of $\chi_{c1}(3872)$ and $\psi(2S)$ production in pPb collisions at $\sqrt{s_{NN}} = 8.16$ TeV", LHCb Note, 2022.

[19] L. Apolinário, Y.-J. Lee, and M. Winn, "Heavy quarks and jets as probes of the QGP", *Prog. Part. Nucl. Phys.* **127** (2022) 103990, doi:10.1016/j.ppnp.2022.103990, arXiv:2203.16352.

[20] F. Colamaria, "Quark-gluon plasma evolution and hadronization", in *The Tenth Annual Conference on Large Hadron Collider Physics (LHCP2022)*. 2022. These proceedings.